

Variational Monte Carlo study of chiral spin liquid in quantum antiferromagnet on the triangular lattice

Wen-Jun Hu^{1,3}, Shou-Shu Gong^{2,3}, and D. N. Sheng³

¹ *Department of Physics and Astronomy, Rice University, Houston, Texas 77005, USA*

² *National High Magnetic Field Laboratory, Florida State University, Tallahassee, Florida 32310, USA*

³ *Department of Physics and Astronomy, California State University, Northridge, California 91330, USA*

By using the Gutzwiller projected fermionic states and the variational Monte Carlo technique, we study the spin-1/2 Heisenberg model with the first-neighbor (J_1), second-neighbor (J_2), and additional scalar chiral interaction $J_\chi \mathbf{S}_i \cdot (\mathbf{S}_j \times \mathbf{S}_k)$ on the triangular lattice. In the non-magnetic phase regime $0.08 \lesssim J_2/J_1 \lesssim 0.16$ of the $J_1 - J_2$ model, recent density-matrix renormalization group studies [Zhu and White, Phys. Rev. B 92, 041105 (2015); Hu, Gong, Zhu, and Sheng, Phys. Rev. B 92, 140403 (2015)] find a possible gapped spin liquid with the signal of a competition between a chiral and a Z_2 spin liquid. Motivated by the DMRG results, we consider the chiral perturbation $J_\chi \mathbf{S}_i \cdot (\mathbf{S}_j \times \mathbf{S}_k)$ in the non-magnetic regime. We find that as J_χ grows, the gapless U(1) Dirac spin liquid, which is the best variational wave function when $J_\chi = 0$, has the instability towards a gapped spin liquid with non-trivial magnetic fluxes and nonzero chiral order. We calculate topological Chern number and ground-state degeneracy, both of which identify this flux state as the chiral spin liquid with fractionalized Chern number $C = 1/2$ and two-fold topological degeneracy. Our results indicate a positive direction to stabilize a chiral spin liquid near the $J_1 - J_2$ model.

PACS numbers: 75.10.Jm, 75.10.Kt, 75.40.Mg, 75.50.Ee

I. INTRODUCTION

Quantum spin liquid is one kind of long-range entangled states without breaking neither spin rotation nor lattice translation symmetries even at zero temperature^{1,2}. The physics of spin liquid has been playing an essential role to understand strongly correlated systems and unconventional superconductivity^{3,4}. The emergent topological order⁵⁻⁷ and fractionalized quasiparticles⁸⁻¹⁰ of spin liquid have wide applications on quantum computations and quantum communications¹¹. In experiment, one of the best candidates to realize spin liquid is frustrated antiferromagnetic material. A natural way to form geometric frustration is to have the corner-sharing triangle and the face-sharing triangle structures on lattice.

The simplest lattice which is constructed from corner-sharing triangles is the kagomé lattice. At experimental side, the most promising materials to realize spin liquid on kagomé lattice are the spin-1/2 antiferromagnets herbertsmithite and kapellasite¹²⁻¹⁷. Theoretically, density-matrix renormalization group (DMRG) studies consistently find a gapped spin liquid in the spin-1/2 kagomé Heisenberg model with the nearest-neighbor (NN) interactions¹⁸⁻²⁰. However, the variational studies based on projected fermionic parton wave functions favor a gapless U(1) Dirac spin liquid (DSL) with competing ground-state energy²¹⁻²⁴. Near the NN model, a robust chiral spin liquid (CSL)^{25,26} is unambiguously established by introducing second- and third-neighbor couplings or chiral interaction²⁷⁻³³. This CSL spontaneously breaks time-reversal symmetry (TRS) and is identified as the $\nu = 1/2$ bosonic fractional quantum Hall state.

On the other hand, the typical system with face-sharing triangles is the simple spin-1/2 triangular lattice systems. The NN Heisenberg antiferromagnetic model

on the triangular lattice is the first candidate proposed to realize a spin liquid³; however, a 120° antiferromagnetic order is found in the subsequent studies³⁴⁻³⁸. Although spin liquid does not exist in the NN model, both experimental and theoretical studies find that the competing interactions may open a new route for realizing such states. In the organic weak Mott insulators with triangular lattice structure such as κ -(ET)₂Cu₂(CN)₃ and EtMe₃Sb[Pd(dmit)₂]₂³⁹⁻⁴⁴, no magnetic order is observed at the temperature much lower than the interaction energy scale. The spin liquid behaviors are explained by a gapless spin Bose metal of a triangular model with four-site ring-exchange couplings⁴⁵⁻⁴⁸. The space anisotropy of the NN couplings has also been studied extensively as a possible mechanism to induce a spin liquid state or a spin spiral phase⁴⁹⁻⁵³. Recently, different theoretical studies consistently find a non-magnetic phase in the $J_1 - J_2$ triangular Heisenberg model between the 120° and the stripe antiferromagnetic phases for $0.08 \lesssim J_2/J_1 \lesssim 0.15$ ⁵⁴⁻⁶². DMRG results find a possible gapped spin liquid in this non-magnetic regime^{58,59}. However, the system appears to have a competition between a spin liquid breaking TRS and the Z_2 spin liquid preserving TRS⁵⁹, which may imply strong finite-size effects in DMRG calculations as the system has difficulty to settle into one state. On the other hand, recent variational Monte Carlo studies⁶² find that the gapless U(1) DSL is the best candidate, whose energy is lower than the variational energies for various Z_2 spin liquids^{63,64}. Here, this non-magnetic regime with various candidate states seems to like the situation of the NN kagomé model, where different perturbations have been considered and a robust CSL is established. Inspired by the competing chiral state found in DMRG⁵⁹, we address the issue that whether a CSL might be stabilized by introducing further

perturbations in $J_1 - J_2$ triangular lattice model.

Motivated by this question, we use the variational Monte Carlo (VMC) calculations based on the flux state of fermionic representation to study the $J_1 - J_2$ triangular Heisenberg model with additional TRS breaking chiral interactions. The model Hamiltonian is defined as

$$H = J_1 \sum_{\langle ij \rangle_{\text{horizontal}}} \mathbf{S}_i \cdot \mathbf{S}_j + J'_1 \sum_{\langle ij \rangle_{\text{zigzag}}} \mathbf{S}_i \cdot \mathbf{S}_j + J_2 \sum_{\langle\langle ij \rangle\rangle} \mathbf{S}_i \cdot \mathbf{S}_j + J_\chi \sum_{\triangle/\nabla} \mathbf{S}_i \cdot (\mathbf{S}_j \times \mathbf{S}_k), \quad (1)$$

where J_1 and J'_1 are the horizontal and zigzag NN couplings, respectively (see Fig. 1(a)). We set $J_1 = 1.0$ as energy scale, and focus on the phase regime with $0.96 \leq J'_1 \leq 1.04$ and $0 \leq J_2 \leq 0.15$. The chiral couplings J_χ have the same magnitude in each triangle (up triangle \triangle and down triangle ∇) as shown in Fig. 1(a), and the sites i , j , and k follow the clockwise order in all triangles. In recent VMC calculations, some topological features of the spin liquids constructed based on fermionic flux states have been obtained^{65–67}. In particular, the VMC studies find the CSL in the extended kagomé model by showing the ground-state degeneracy and topological Chern number³². In our calculations, we will follow these techniques.

Through our VMC calculations, we find that while the 120° antiferromagnetic order vanishes at a finite chiral coupling J_χ for $J_2 \lesssim 0.08$, the gapless U(1) DSL in the non-magnetic regime $0.08 \lesssim J_2 \lesssim 0.15$ has the instability towards a CSL as soon as we turn on the J_χ term. This CSL has a quantized topological Chern number $C = 1/2$ and two-fold topological degenerate ground states, which characterize the CSL as the $\nu = 1/2$ fractional quantum Hall state. We also study the relation between the chiral order and the lattice anisotropy of J_1 coupling in the CSL phase regime. We find the consistent behaviors with the DMRG results⁵⁹ that some spin coupling anisotropy may enhance the robustness of the CSL. Our VMC results indicate a positive direction to stabilize a CSL near the non-magnetic phase in the $J_1 - J_2$ triangular Heisenberg model.

II. VARIATIONAL WAVE FUNCTIONS

Following one of the novel ways to construct spin liquid states beyond the mean-field level, we introduce the projected fermionic wave functions for our variational calculations⁶⁸. In this representation, spin operator \mathbf{S}_i is expressed using the spinon operators as $\mathbf{S}_i = \frac{1}{2} c_{i,\alpha}^\dagger \boldsymbol{\sigma}_{\alpha\beta} c_{i,\beta}$, where $\boldsymbol{\sigma} = (\sigma^x, \sigma^y, \sigma^z)$ is the Pauli matrices and $c_{i,\sigma}^\dagger$ ($c_{i,\sigma}$) creates (annihilates) an electron with spin σ at site i . Therefore, the Hamiltonian Eq. (1) could be represented using the fermionic operators, and the Gutzwiller projector $\mathcal{P}_G = \prod_i (1 - n_{i\uparrow} n_{i\downarrow})$ is introduced to enforce no double occupation on each site. For the variational

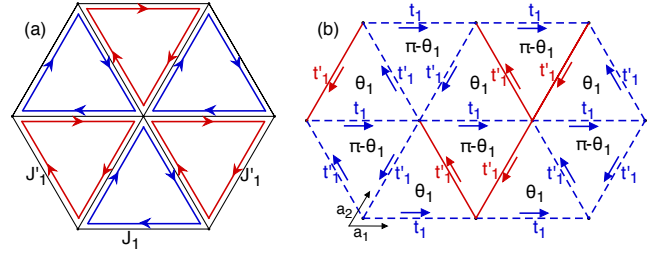


FIG. 1: (Color online) Model Hamiltonian and variational *Ansatz*. (a) In the $J_1 - J'_1 - J_2 - J_\chi$ model Eq.(1), we add the same J_χ in the up (blue) and down (red) triangles. (b) The variational *Ansatz* with the NN hopping t_1 and t'_1 is shown. Solid (dashed) lines indicate positive (negative) hoppings, which define the U(1) DSL. The phases ϕ_1 and ϕ'_1 are added upon this *Ansatz* to obtain a CSL. The direction of arrows indicates one possible convention of phases. In each up triangle, the flux is $\theta_1 = \phi_1 + 2\phi'_1$; in each down triangle, the flux is $\theta_2 = \pi - \theta_1$.

calculations, we define the variational wave function as

$$|\Psi_v\rangle = \mathcal{J}_s \mathcal{P}_G |\Psi_0\rangle, \quad (2)$$

where $\mathcal{J}_s = \exp(1/2 \sum_{ij} v_{ij} S_i^z S_j^z)$ is the spin Jastrow factor with the variational parameters v_{ij} that depend upon distance between sites i and j . $|\Psi_0\rangle$ is an uncorrelated ground state of mean-field Hamiltonian. In the previous VMC calculations of the $J_1 - J_2$ Heisenberg model^{62,63}, the Z_2 spin liquids have the higher energy than the gapless U(1) DSL in the intermediate J_2 regime ($0.08 < J_2 < 0.16$); thus, we consider the mean-field Hamiltonian only with the NN hopping term consistent with the DSL,

$$\mathcal{H}_{\text{MF}} = \sum_{\langle i,j \rangle, \sigma} t_{ij} c_{i,\sigma}^\dagger c_{j,\sigma} + h.c. \quad (3)$$

As shown in Fig. 1(b), the solid (dashed) bonds denote the positive (negative) signs of t_{ij} , which define a magnetic flux $\Phi = 0$ crossing up triangles and $\Phi = \pi$ crossing down triangles (or opposite)^{62–64}. Thus, the unit cell is doubled in this DSL. In our studies considering bond anisotropy and CSL, we allow the anisotropy of the NN hopping t_{ij} and t'_{ij} with both real and imaginary parts, i.e., $t_{ij} = |t_{ij}| e^{i\phi_{ij}}$. In Fig. 1(b), we show the *Ansatz* of the variational wave function.⁶⁹ Since the requirement of $t_{ij}^* = t_{ji}$, we define the orientation of the hopping terms in this way: for the hopping from j to i , t_{ij} (t'_{ij}) has the direction (opposite direction) along the arrow shown in Fig. 1(b). Here, we choose the definition that the up triangles have the fluxes $\theta_1 = \phi_1 + 2\phi'_1$, and the down triangles have the fluxes $\theta_2 = \pi - \theta_1$. Such a state can be denoted as $[\theta_1, \pi - \theta_1]$. Thus, using this symbol, the U(1) DSL has the fluxes $[0, \pi]$, and the wave functions with non-zero θ_1 describe the states with spin chirality⁵.

We will also consider the effect of J_χ to the 120° Néel order for $J_2 \lesssim 0.08$. In this case, we define the magnetic

states as

$$\mathcal{H}_{\text{MAG}} = \sum_{\langle i,j \rangle, \sigma} (t_{ij} c_{i,\sigma}^\dagger c_{j,\sigma} + h.c.) + h \sum_i \mathbf{M}_i \cdot \mathbf{S}_i, \quad (4)$$

where the magnetic order is described by variational parameter h and vector \mathbf{M}_i . The magnetic long-range order is directly related to a non-zero h . For describing the 120° Néel state, we set $\mathbf{M}_i = (\cos(\mathbf{r}_i \cdot \mathbf{q} + \eta_i), \sin(\mathbf{r}_i \cdot \mathbf{q} + \eta_i), 0)$ (\mathbf{q} is the pitch vector and η_i is the phase shift for the sites within the same unit cell) with $\mathbf{q} = (4\pi/3, 0)$. For the vector \mathbf{M}_i in XY plane, the spin Jastrow factor $\mathcal{J}_s = \exp(1/2 \sum_{ij} v_{ij} S_i^z S_j^z)$ correctly describes spin fluctuations around the classical spin state.

In this paper we study the competitions among the 120° Néel state, the gapless $U(1)$ DSL, and the gapped CSL. We perform variational calculations at half filling on toric clusters with $L \times L$ sites under the periodic/antiperiodic boundary conditions (PBC/APBC). In order to find the energetically favored state, we use the stochastic reconfiguration (SR) optimization method⁷⁰ to optimize the variational parameters.

III. COMPETITION BETWEEN MAGNETIC AND CHIRAL ORDERS

First of all, we study the competition between the magnetic and chiral orders for $J_2 \lesssim 0.08$. When $J_\chi = 0$, the system has the 120° Néel order. When J_χ is much larger than J_1 coupling, the classical spin analyses show that the system would become a non-coplanar tetrahedral state with four sublattices, where the spins of four sublattices point toward the corners of a tetrahedron⁷¹. Therefore, we expect a phase diagram like either “ 120° Néel - tetrahedral” or “ 120° Néel - intermediate phase - tetrahedral”. Interestingly, the CSL discovered in the kagomé model emerges between a 120° Néel phase and

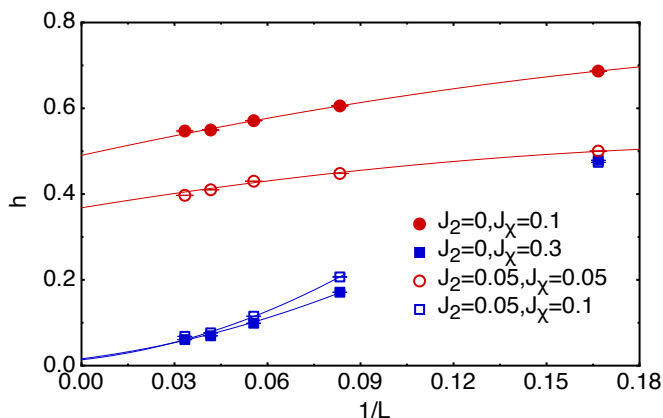


FIG. 2: (Color online) Finite-size scaling of the magnetic order variational parameter h for $J_2 = 0$ and 0.05 . We use the $L \times L$ toric clusters with PBC at $L = 6, 12, 18, 24, 30$. Quadratic fittings are used for all the data.

the non-coplanar cuboc phase³⁰. In our present studies, we do not include the variational wave function of the tetrahedral state. Thus, we only consider the vanishing of the 120° Néel order with the increase of J_χ (we expect further studies using unbiased methods to investigate the phase transition between the 120° Néel and the tetrahedral phases in the future work).

In our variational calculations for $J_2 \lesssim 0.08$, we start from the wave function Eq. (4) and optimize the parameter h and Jastrow factor v_{ij} . $h = 0$ describes the vanished Néel order. We study the lattice with $L = 6, 12, 18, 24, 30$, where the 120° Néel order is not frustrated by boundary conditions. In Fig. 2, we show the variational parameter h of magnetic order for $J_2 = 0$ and 0.05 with J_χ on different clusters. For both J_2 couplings with small J_χ , the variational parameter h decreases quite slowly with increasing system sizes and smoothly extrapolates to a finite value in the thermodynamic limit. When J_χ is large enough ($J_\chi \gtrsim 0.1$), the magnetic order parameter h decreases sharply and scales to vanishing when $L \rightarrow \infty$. Our results clearly indicate that there is a phase transition with vanished 120° Néel order at a finite J_χ .

IV. CHIRAL SPIN LIQUID EMERGING NEAR THE GAPLESS DIRAC SPIN LIQUID

In this section we study the possible CSL near the gapless $U(1)$ DSL. We start from the non-magnetic variational wave function Eq. (3) without magnetic term ($h = 0$) and spin Jastrow factor ($v_{ij} = 0$). Thus, the variational parameters are the imaginary part of t_1 and both real and imaginary parts of t'_1 . We will focus our studies for $J_2 = 0.1$.

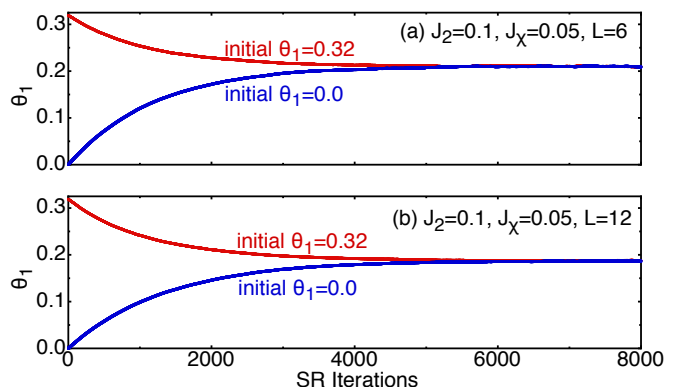


FIG. 3: (Color online) The variational Monte Carlo optimizations of the flux $\theta_1 = 3 \arctan(\text{Im}(t_1)/\text{Re}(t_1))$ are shown for $J_2 = 0.1$ and $J_\chi = 0.05$ on $L = 6$ (a) and 12 (b) clusters. Different initial values $\theta_1 = 0.32$ ($\text{Im}(t_1) = 0.107$) and 0 are chosen.

A. Isotropic system with $J_1 = J'_1$

1. Optimization and measurement of local order parameters

For the isotropic system with $J_1 = J'_1$, we have $t_1 = t'_1$, and the only variational parameter is the imaginary part of the NN hopping. Before discussing the results, we demonstrate the good convergence of our calculations. In Fig. 3, we show the optimization of θ_1 for $J_2 = 0.1$, $J_\chi = 0.05$ on the 6×6 and 12×12 clusters. We obtain the converged θ_1 after optimization, which are found to be independent of initial values.

To study the CSL, we optimize the variational wave function for different J_χ on different system size with L up to $L = 30$. On the $L = 6$ and $L = 12$ clusters, we study the system with J_χ up to 0.3. As shown in Fig. 4, the optimized flux θ_1 increases with the growing J_χ . For $J_\chi = 0.02, 0.05, 0.1$, we study the larger clusters, which give the optimized θ_1 that almost do not change with increasing system size. In the inset of Fig. 4, we also show the finite-size scaling of the ground-state energy for small J_χ , which support the good convergence of the calculations with system size.

With the optimized finite variational parameter θ_1 , we expect non-zero chiral order of the optimized wave function, which can be measured through the three spins scalar chirality in each triangle as:

$$\langle \chi \rangle = \langle \mathbf{S}_1 \cdot (\mathbf{S}_2 \times \mathbf{S}_3) \rangle. \quad (5)$$

In our calculations, we find that the chiral order parameter $\langle \chi \rangle$ of the up and down triangles are the same within the error bar. In Fig. 5, we show $\langle \chi \rangle$ as a function of the chiral coupling J_χ on different clusters up to $L = 30$, which grows continuously with increasing J_χ . The finite-size scaling in the inset of Fig. 5 clearly demonstrates the non-zero chirality in the thermodynamic limit.

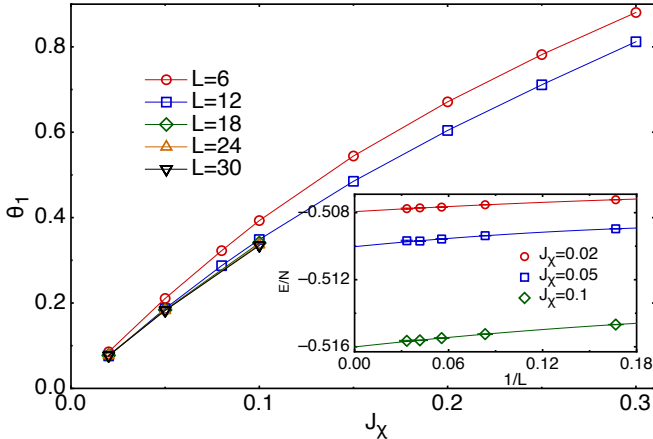


FIG. 4: (Color online) The optimized flux θ_1 in the variational wave function at $J_2 = 0.1$ with different J_χ on $L = 6, 12, 18, 24$, and 30 clusters. The inset is the finite size scaling for the ground state energy at $J_\chi = 0.02, 0.05$, and 0.1 .

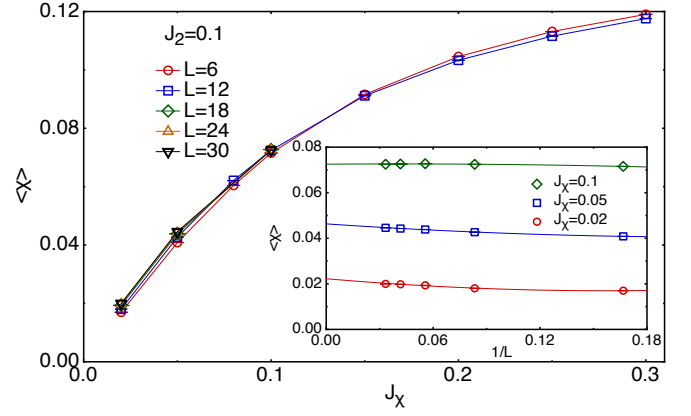


FIG. 5: (Color online) The chiral order parameter $\langle \chi \rangle$ of the optimized wave functions. For the up and down triangles, we obtain the same value of $\langle \chi \rangle$ within the error bar. The inset is the finite size scaling for the chirality $\langle \chi \rangle$ at $J_\chi = 0.02, 0.05$, and 0.1 .

2. Topological properties

In order to characterize the non-trivial topological properties of the chiral state, we calculate the topological Chern number and the ground state degeneracy.

In our calculations, the topological Chern number is computed as the integral over the Berry curvature $F(\Theta_1, \Theta_2)$ in boundary phase space:^{72–75}

$$C = \frac{1}{2\pi} \int d\Theta_1 d\Theta_2 F(\Theta_1, \Theta_2), \quad (6)$$

where $0 \leq \Theta_k \leq 2\pi$ ($k = 1, 2$) are twist boundary phases for the torus systems. To obtain this integral, we uniformly divide the boundary phase space into M plaquettes (M is chosen up to 100). The Berry curvature defined for each plaquette l is calculated as $F_l = \arg \prod_{i=1}^4 \langle \Psi_V^{l_{i+1}} | \Psi_V^{l_i} \rangle$ ($l = 1, \dots, M$). The label i ($i = 1, 2, 3, 4$) denotes the four corners of the l -th plaquette, where the periodic condition requires $\Psi_V^{l_5} = \Psi_V^{l_1}$. The wave function $|\Psi_V^l\rangle$ is the optimized wave function of the mean-field Hamiltonian with twisted boundary conditions, which have the opposite requirements for the spin up and spin down partons, namely $c_{j+L_k\uparrow} = c_{j\uparrow} e^{i\Theta_k}$ and $c_{j+L_k\downarrow} = c_{j\downarrow} e^{-i\Theta_k}$ ($k = 1$ and 2 , and $L_1 = L_2 = L$ in our calculations). The overlap for the Berry curvature $\langle \Psi_V^{l_{i+1}} | \Psi_V^{l_i} \rangle = \sum_x P(x) \frac{\langle x | \Psi_V^{l_i} \rangle}{\langle x | \Psi_V^{l_{i+1}} \rangle}$ is calculated by variational Monte Carlo method according to the weight $P(x) = \frac{|\langle x | \Psi_V^{l_{i+1}} \rangle|^2}{\sum_x |\langle x | \Psi_V^{l_{i+1}} \rangle|^2}$. We obtain the Berry curvatures as shown in Fig. 6. Here, we consider two wave functions. One is the optimized state at $J_2 = 0.1$, $J_\chi = 0.05$ (fluxes is obtained as $\theta_1 \approx 0.18$), and the other one for comparison is the state with fluxes $[\pi/2, \pi/2]$. For both states, we do the integration of the Berry curvature from 0 to 2π . We must emphasize that the integration from 0

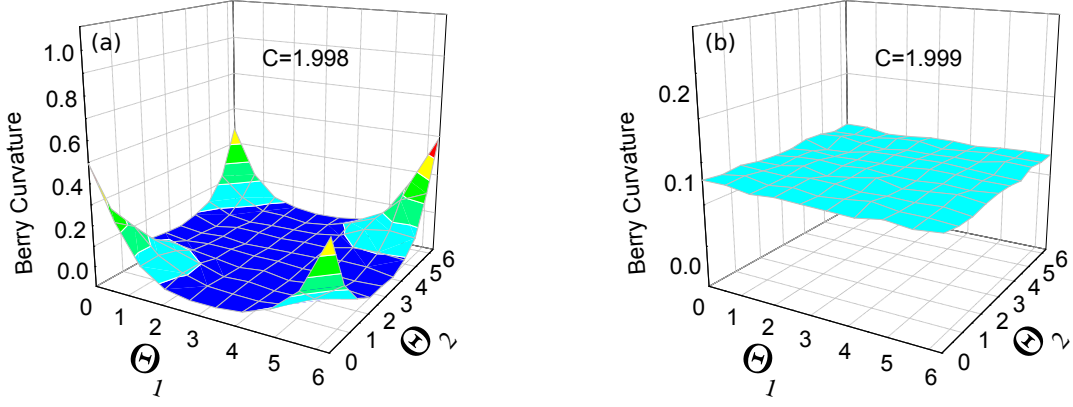


FIG. 6: (Color online) Berry curvature for the states of (a) $J_2 = 0.1, J_\chi = 0.05$ on the $L = 12$ lattice and (b) $[\pi/2, \pi/2]$ on the $L = 8$ lattice. For both calculations, the Brillouin zone is divided into a mesh with 100 plaquettes. The summation between 0 and 2π gives $C = 1.998$ (a) and 1.999 (b).

to 2π for the operators of two partons (with spin up and spin down) includes two periods of phases for the spin operators, so the final results of the Chern number must be divided by 4 for the spin system. In our calculations, the integrations between 0 and 2π for both states give the results 2 with high accuracy, which leads to a Chern number $C = 1/2$.

In the variational approach with Gutzwiller projected parton construction, the degeneracy of the wave function is consistent with number of the linear independence states of the fermionic variational wave functions according to the SU(2) Chern-Simons theory.^{65–67} The idea^{65–67} is that through changing the boundary conditions of the mean field Hamiltonian to either periodic or antiperiodic in \vec{a}_1 and \vec{a}_2 directions (see Fig. 1(b)), we can obtain four projected states denoted as $|\psi_1, \psi_2\rangle$. We label $\psi_i = 0$ for periodic boundary condition and π for antiperiodic boundary condition ($i = 1, 2$), i.e., these four projected states are $\{|0, 0\rangle, |0, \pi\rangle, |\pi, 0\rangle, |\pi, \pi\rangle\}$. Then we can calculate the overlaps between any two of the four states to obtain the overlap matrix^{65–67}, and the number of the nonzero eigenvalues of this overlap matrix gives the number of the linearly independent states. Based on the experience of the similar calculations on kagomé antiferromagnet³², we should choose a state with a big mean-field band gap to suppress the strong finite-size effects on small clusters. Thus, we calculate the overlap matrix on the 8×8 cluster for the state with flux $\theta_1 = \pi/2$ (this state has a big mean-field band gap 4.1), and obtain the overlap matrix \mathcal{O} as

$$\begin{aligned} \mathcal{O} &= \begin{pmatrix} \langle 0, 0|0, 0\rangle & \langle 0, 0|0, \pi\rangle & \langle 0, 0|\pi, 0\rangle & \langle 0, 0|\pi, \pi\rangle \\ \langle 0, \pi|0, 0\rangle & \langle 0, \pi|0, \pi\rangle & \langle 0, \pi|\pi, 0\rangle & \langle 0, \pi|\pi, \pi\rangle \\ \langle \pi, 0|0, 0\rangle & \langle \pi, 0|0, \pi\rangle & \langle \pi, 0|\pi, 0\rangle & \langle \pi, 0|\pi, \pi\rangle \\ \langle \pi, \pi|0, 0\rangle & \langle \pi, \pi|0, \pi\rangle & \langle \pi, \pi|\pi, 0\rangle & \langle \pi, \pi|\pi, \pi\rangle \end{pmatrix} \\ &\approx \begin{pmatrix} 1 & 0.57 & 0.57 & 0.58 \\ 0.57 & 1 & 0.58e^{-i1.59} & 0.58e^{i1.59} \\ 0.57 & 0.58e^{i1.59} & 1 & 0.58e^{-i1.59} \\ 0.57 & 0.58e^{-i1.59} & 0.58e^{i1.58} & 1 \end{pmatrix} \\ &\approx \begin{pmatrix} 1 & \frac{1}{\sqrt{3}} & \frac{1}{\sqrt{3}} & \frac{1}{\sqrt{3}} \\ \frac{1}{\sqrt{3}} & 1 & -\frac{i}{\sqrt{3}} & \frac{i}{\sqrt{3}} \\ \frac{1}{\sqrt{3}} & \frac{i}{\sqrt{3}} & 1 & -\frac{i}{\sqrt{3}} \\ \frac{1}{\sqrt{3}} & -\frac{i}{\sqrt{3}} & \frac{i}{\sqrt{3}} & 1 \end{pmatrix}. \end{aligned} \quad (7)$$

In this calculation, we fix the global phases in such a way that all the overlaps with $|0, 0\rangle$ are set to real. The number of the independent ground states can be found by diagonalizing the overlap matrix, i.e., $\mathcal{O} = U^\dagger \Lambda U$. We find that only two eigenvalues are non-zero, which indicates that only two eigenvectors are linearly independent. This fact implies that the ground-state degeneracy is two-fold. Our calculations of topological Chern number and ground state degeneracy consistently suggest that this chiral state is the $\nu = 1/2$ Laughlin state.

B. Anisotropic system with $J_1 \neq J'_1$

In the DMRG studies on the $J_1 - J_2$ triangular model, a weak chiral order is found on the finite-size system in the even sector, and by tuning the bond anisotropy J_1 and J'_1 (J_1 and J'_1 are along the vertical and the zigzag directions, respectively) the chiral order seems to enhance with $J_1 - J'_1$ for $0.96 \lesssim J'_1/J_1 \lesssim 1.04$ ⁵⁹. The bond anisotropy and chiral order appear to have interesting competition. In this part, we introduce the bond

spatial anisotropy in the $J_1-J_2-J_\chi$ model to study this competition. We choose $J_2 = J_\chi = 0.1$ and change the anisotropy J'_1 from 0.96 to 1.04. Correspondingly, we use the variational wave function with $t_1 \neq t'_1$ (see Fig. 1(b)). Thus, there are three variational parameters (imaginary part of t_1 , real and imaginary parts of t'_1), including two fluxes that need to be optimized. Since the optimizations with two fluxes are very time consuming, we only did variational calculations on the $L = 12$ and 18 clusters.

As shown in Fig. 7(a), we find that once $J'_1 \neq J_1$, we obtain $|t_1| \neq |t'_1|$ after optimization, which indicates that the optimized wave functions break lattice rotational symmetry. Then, we measure the spin chirality $\langle \chi \rangle$ for different J'_1 . Interestingly, as shown in Fig. 7(b), we find that when $J'_1 < J_1$, the chiral order is enhanced with increasing anisotropy $|J_1 - J'_1|$; on the contrary when $J'_1 > J_1$, chiral order is suppressed with increasing $|J_1 - J'_1|$.

V. CONCLUSIONS

We have studied the spin-1/2 antiferromagnetic J_1-J_2 Heisenberg model with additional chiral coupling $J_\chi \mathbf{S}_i \cdot (\mathbf{S}_j \times \mathbf{S}_k)$ on the triangular lattice. By performing the variational Monte Carlo simulations and considering different variational wave functions, we find that while the 120° Néel order vanishes at a finite J_χ , and the gapless U(1) Dirac spin liquid in the intermediate regime would become a chiral spin liquid once J_χ starts to grow. By calculating the topological Chern number and ground-state degeneracy, we identify this CSL as the $\nu = 1/2$ Laughlin state. We also consider the relation between the chiral order and the spacial anisotropy in the model, and we find that the chiral order can be enhanced

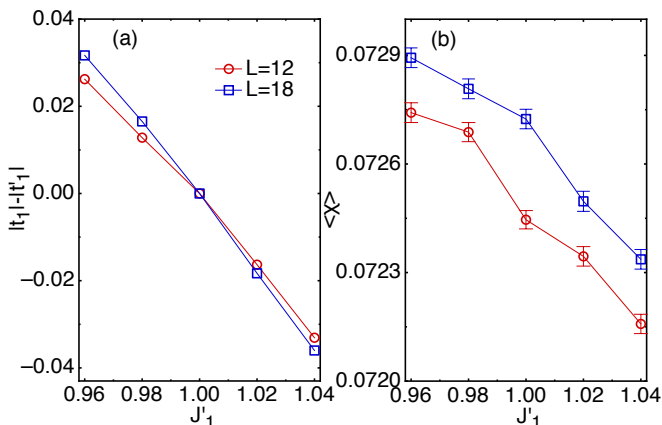


FIG. 7: (Color online). Variational results for the anisotropic system with $J_1 \neq J'_1$. (a) The difference of the hoppings along horizontal and zigzag directions for $0.96 \leq J'_1 \leq 1.04$ on $L = 12$ and 18 clusters at $J_2 = 0.1$ and $J_\chi = 0.1$. (b) The chiral order parameter $\langle \chi \rangle$ as function of anisotropy J'_1 on $L = 12$ and 18 clusters at $J_2 = 0.1$ and $J_\chi = 0.1$.

(suppressed) when the anisotropic parameter $J'_1 < J_1$ ($J'_1 > J_1$), which is consistent with the DMRG observation. Our results suggest a new way to stabilize a chiral spin liquid near the $J_1 - J_2$ triangular model. Finally we would like to mention that we have not considered all the possible variational states, and it is worth to use unbiased numerical simulations such as DMRG to clarify the phase diagram and the properties of the ground states.

ACKNOWLEDGMENTS

We acknowledge stimulating discussions with O. I. Motrunich, A. Nevidomskyy and S. Bieri. This research is supported by the National Science Foundation through Grants No. DMR-1408560 (W.-J.H., D.N.S.) and PREM DMR-1205734 (S.S.G.) at CSUN, NSF Grant No. DMR-1350237 and DMR-1309531 at Rice (W.-J.H.), and the National High Magnetic Field Laboratory that is supported by NSF DMR-1157490 and the State of Florida (S.S.G.).

- ¹ L. Balents, Nature (London) **464**, 199 (2010), URL <http://www.nature.com/nature/journal/v464/n7286/full/nature08917.html>.
- ² L. Savary and L. Balents, ArXiv e-prints (2016), 1601.03742, URL <http://arxiv.org/abs/1601.03742>.
- ³ P. W. Anderson, Mater. Res. Bull. **8**, 153 (1973), URL <http://www.sciencedirect.com/science/article/pii/0025540873901670>.
- ⁴ P. A. Lee, N. Nagaosa, and X.-G. Wen, Rev. Mod. Phys. **78**, 17 (2006), URL <http://link.aps.org/doi/10.1103/RevModPhys.78.17>.
- ⁵ X. G. Wen, Phys. Rev. B **40**, 7387 (1989), URL <http://link.aps.org/doi/10.1103/PhysRevB.40.7387>.
- ⁶ X. G. Wen and Q. Niu, Phys. Rev. B **41**, 9377 (1990), URL <http://link.aps.org/doi/10.1103/PhysRevB.41.9377>.
- ⁷ X.-G. Wen, International Journal of Modern Physics B **4**, 239 (1990), URL <http://www.worldscientific.com/doi/abs/10.1142/S0217979290000139>.
- ⁸ X. G. Wen, Phys. Rev. B **44**, 2664 (1991), URL <http://link.aps.org/doi/10.1103/PhysRevB.44.2664>.
- ⁹ T. Senthil and M. P. A. Fisher, Phys. Rev. B **62**, 7850 (2000), URL <http://link.aps.org/doi/10.1103/PhysRevB.62.7850>.
- ¹⁰ T. Senthil and M. P. A. Fisher, Phys. Rev. Lett. **86**, 292 (2001), URL <http://link.aps.org/doi/10.1103/PhysRevLett.86.292>.
- ¹¹ A. Kitaev, Annals of Physics **321**, 2 (2006), URL <http://www.sciencedirect.com/science/article/pii/S0003491605002381>.
- ¹² P. Mendels, F. Bert, M. A. de Vries, A. Olariu, A. Harrison, F. Duc, J. C. Trombe, J. S. Lord, A. Amato, and C. Baines, Phys. Rev. Lett. **98**, 077204 (2007), URL <http://link.aps.org/doi/10.1103/PhysRevLett.98.077204>.
- ¹³ J. S. Helton, K. Matan, M. P. Shores, E. A. Nytko, B. M. Bartlett, Y. Yoshida, Y. Takano, A. Suslov, Y. Qiu, J.-H. Chung, et al., Phys. Rev. Lett. **98**, 107204 (2007), URL <http://link.aps.org/doi/10.1103/PhysRevLett.98.107204>.
- ¹⁴ M. A. de Vries, J. R. Stewart, P. P. Deen, J. O. Piatek, G. J. Nilsen, H. M. Rønnow, and A. Harrison, Phys. Rev. Lett. **103**, 237201 (2009), URL <http://link.aps.org/doi/10.1103/PhysRevLett.103.237201>.
- ¹⁵ B. Fåk, E. Kermarrec, L. Messio, B. Bernu, C. Lhuillier, F. Bert, P. Mendels, B. Koteswararao, F. Bouquet, J. Ollivier, et al., Phys. Rev. Lett. **109**, 037208 (2012), URL <http://link.aps.org/doi/10.1103/PhysRevLett.109.037208>.
- ¹⁶ T.-H. Han, J. S. Helton, S. Chu, D. G. Nocera, J. A. Rodriguez-Rivera, C. Broholm, and Y. S. Lee, Nature (London) **492**, 406 (2012), URL <http://www.nature.com/nature/journal/v492/n7429/full/nature11659.html>.
- ¹⁷ M. Fu, T. Imai, T.-H. Han, and Y. S. Lee, Science **350**, 655 (2015), URL <http://science.sciencemag.org/content/350/6261/655.short>.
- ¹⁸ S. Yan, D. A. Huse, and S. R. White, Science **332**, 1173 (2011), URL <http://www.sciencemag.org/content/332/6034/1173.full>.
- ¹⁹ S. Depenbrock, I. P. McCulloch, and U. Schollwöck, Phys. Rev. Lett. **109**, 067201 (2012), URL <http://link.aps.org/doi/10.1103/PhysRevLett.109.067201>.
- ²⁰ H.-C. Jiang, Z. Wang, and L. Balents, Nature Physics **8**, 902 (2012), URL <http://www.nature.com/nphys/journal/v8/n12/full/nphys2465.html>.
- ²¹ Y. Ran, M. Hermele, P. A. Lee, and X.-G. Wen, Phys. Rev. Lett. **98**, 117205 (2007), URL <http://link.aps.org/doi/10.1103/PhysRevLett.98.117205>.
- ²² Y. Iqbal, F. Becca, and D. Poilblanc, Phys. Rev. B **84**, 020407 (2011), URL <http://link.aps.org/doi/10.1103/PhysRevB.84.020407>.
- ²³ Y. Iqbal, F. Becca, S. Sorella, and D. Poilblanc, Phys. Rev. B **87**, 060405 (2013), URL <http://link.aps.org/doi/10.1103/PhysRevB.87.060405>.
- ²⁴ Y. Iqbal, D. Poilblanc, and F. Becca, Phys. Rev. B **89**, 020407 (2014), URL <http://link.aps.org/doi/10.1103/PhysRevB.89.020407>.
- ²⁵ V. Kalmeyer and R. B. Laughlin, Phys. Rev. Lett. **59**, 2095 (1987), URL <http://link.aps.org/doi/10.1103/PhysRevLett.59.2095>.
- ²⁶ X. G. Wen, F. Wilczek, and A. Zee, Phys. Rev. B **39**, 11413 (1989), URL <http://link.aps.org/doi/10.1103/PhysRevB.39.11413>.
- ²⁷ L. Messio, B. Bernu, and C. Lhuillier, Phys. Rev. Lett. **108**, 207204 (2012), URL <http://link.aps.org/doi/10.1103/PhysRevLett.108.207204>.
- ²⁸ S.-S. Gong, W. Zhu, and D. Sheng, Scientific reports **4**, 6317 (2014), URL <http://www.nature.com/srep/2014/140910/srep06317/full/srep06317.html>.
- ²⁹ Y.-C. He, D. N. Sheng, and Y. Chen, Phys. Rev. Lett. **112**, 137202 (2014), URL <http://link.aps.org/doi/10.1103/PhysRevLett.112.137202>.
- ³⁰ S.-S. Gong, W. Zhu, L. Balents, and D. N. Sheng, Phys. Rev. B **91**, 075112 (2015), URL <http://link.aps.org/doi/10.1103/PhysRevB.91.075112>.
- ³¹ B. Bauer, L. Cincio, B. P. Keller, M. Dolfi, G. Vidal, S. Trebst, and A. W. W. Ludwig, Nature Communications **5**, 5137 (2014), URL <http://www.nature.com/ncomms/2014/141010/ncomms6137/abs/ncomms6137.html>.
- ³² W.-J. Hu, W. Zhu, Y. Zhang, S. Gong, F. Becca, and D. N. Sheng, Phys. Rev. B **91**, 041124 (2015), URL <http://link.aps.org/doi/10.1103/PhysRevB.91.041124>.
- ³³ A. Wietek, A. Sterdyniak, and A. M. Läuchli, Phys. Rev. B **92**, 125122 (2015), URL <http://link.aps.org/doi/10.1103/PhysRevB.92.125122>.
- ³⁴ S. Sachdev, Phys. Rev. B **45**, 12377 (1992), URL <http://link.aps.org/doi/10.1103/PhysRevB.45.12377>.
- ³⁵ B. Bernu, C. Lhuillier, and L. Pierre, Phys. Rev. Lett. **69**, 2590 (1992), URL <http://link.aps.org/doi/10.1103/PhysRevLett.69.2590>.
- ³⁶ L. Capriotti, A. E. Trumper, and S. Sorella, Phys. Rev. Lett. **82**, 3899 (1999), URL <http://link.aps.org/doi/10.1103/PhysRevLett.82.3899>.
- ³⁷ W. Zheng, J. O. Fjærestad, R. R. P. Singh, R. H. McKenzie, and R. Coldea, Phys. Rev. B **74**, 224420 (2006), URL <http://link.aps.org/doi/10.1103/PhysRevB.74.224420>.
- ³⁸ S. R. White and A. L. Chernyshev, Phys. Rev. Lett. **99**, 127004 (2007), URL <http://link.aps.org/doi/10.1103/PhysRevLett.99.127004>.
- ³⁹ Y. Shimizu, K. Miyagawa, K. Kanoda, M. Maesato, and G. Saito, Phys. Rev. Lett. **91**, 107001 (2003), URL <http://link.aps.org/doi/10.1103/PhysRevLett.91.107001>.

- ⁴⁰ Y. Kurosaki, Y. Shimizu, K. Miyagawa, K. Kanoda, and G. Saito, Phys. Rev. Lett. **95**, 177001 (2005), URL <http://link.aps.org/doi/10.1103/PhysRevLett.95.177001>.
- ⁴¹ S. Yamashita, Y. Nakazawa, M. Oguni, Y. Oshima, H. Nojiri, Y. Shimizu, K. Miyagawa, and K. Kanoda, Nature Physics **4**, 459 (2008), URL <http://www.nature.com/nphys/journal/v4/n6/abs/nphys942.html>.
- ⁴² M. Yamashita, N. Nakata, Y. Kasahara, T. Sasaki, N. Yoneyama, N. Kobayashi, S. Fujimoto, T. Shibauchi, and Y. Matsuda, Nature Physics **5**, 44 (2009), URL <http://www.nature.com/nphys/journal/v5/n1/full/nphys1134.html>.
- ⁴³ T. Itou, A. Oyamada, S. Maegawa, M. Tamura, and R. Kato, Phys. Rev. B **77**, 104413 (2008), URL <http://link.aps.org/doi/10.1103/PhysRevB.77.104413>.
- ⁴⁴ M. Yamashita, N. Nakata, Y. Senshu, M. Nagata, H. M. Yamamoto, R. Kato, T. Shibauchi, and Y. Matsuda, Science **328**, 1246 (2010), URL <http://www.sciencemag.org/content/328/5983/1246.full>.
- ⁴⁵ O. I. Motrunich, Phys. Rev. B **72**, 045105 (2005), URL <http://link.aps.org/doi/10.1103/PhysRevB.72.045105>.
- ⁴⁶ D. N. Sheng, O. I. Motrunich, and M. P. A. Fisher, Phys. Rev. B **79**, 205112 (2009), URL <http://link.aps.org/doi/10.1103/PhysRevB.79.205112>.
- ⁴⁷ M. S. Block, R. V. Mishmash, R. K. Kaul, D. N. Sheng, O. I. Motrunich, and M. P. A. Fisher, Phys. Rev. Lett. **106**, 046402 (2011), URL <http://link.aps.org/doi/10.1103/PhysRevLett.106.046402>.
- ⁴⁸ G. Misguich, C. Lhuillier, B. Bernu, and C. Waldtmann, Phys. Rev. B **60**, 1064 (1999), URL <http://link.aps.org/doi/10.1103/PhysRevB.60.1064>.
- ⁴⁹ S. Yunoki and S. Sorella, Phys. Rev. B **74**, 014408 (2006), URL <http://link.aps.org/doi/10.1103/PhysRevB.74.014408>.
- ⁵⁰ M. Q. Weng, D. N. Sheng, Z. Y. Weng, and R. J. Bursill, Phys. Rev. B **74**, 012407 (2006), URL <http://link.aps.org/doi/10.1103/PhysRevB.74.012407>.
- ⁵¹ O. A. Starykh and L. Balents, Phys. Rev. Lett. **98**, 077205 (2007), URL <http://link.aps.org/doi/10.1103/PhysRevLett.98.077205>.
- ⁵² A. Weichselbaum and S. R. White, Phys. Rev. B **84**, 245130 (2011), URL <http://link.aps.org/doi/10.1103/PhysRevB.84.245130>.
- ⁵³ E. Ghorbani, L. F. Tocchio, and F. Becca, Phys. Rev. B **93**, 085111 (2016), URL <http://link.aps.org/doi/10.1103/PhysRevB.93.085111>.
- ⁵⁴ L. O. Manuel and H. A. Ceccatto, Phys. Rev. B **60**, 9489 (1999), URL <http://link.aps.org/doi/10.1103/PhysRevB.60.9489>.
- ⁵⁵ R. V. Mishmash, J. R. Garrison, S. Bieri, and C. Xu, Phys. Rev. Lett. **111**, 157203 (2013), URL <http://link.aps.org/doi/10.1103/PhysRevLett.111.157203>.
- ⁵⁶ R. Kaneko, S. Morita, and M. Imada, Journal of the Physical Society of Japan **83** (2014), URL <http://journals.jps.jp/doi/abs/10.7566/JPSJ.83.093707>.
- ⁵⁷ P. H. Y. Li, R. F. Bishop, and C. E. Campbell, Phys. Rev. B **91**, 014426 (2015), URL <http://link.aps.org/doi/10.1103/PhysRevB.91.014426>.
- ⁵⁸ Z. Zhu and S. R. White, Phys. Rev. B **92**, 041105 (2015), URL <http://link.aps.org/doi/10.1103/PhysRevB.92.041105>.
- ⁵⁹ W.-J. Hu, S.-S. Gong, W. Zhu, and D. N. Sheng, Phys. Rev. B **92**, 140403 (2015), URL <http://link.aps.org/doi/10.1103/PhysRevB.92.140403>.
- ⁶⁰ S. N. Saadatmand, B. J. Powell, and I. P. McCulloch, Phys. Rev. B **91**, 245119 (2015), URL <http://link.aps.org/doi/10.1103/PhysRevB.91.245119>.
- ⁶¹ R. F. Bishop and P. H. Y. Li, EPL (Europhysics Letters) **112**, 67002 (2015), URL <http://stacks.iop.org/0295-5075/112/i=6/a=67002>.
- ⁶² Y. Iqbal, W.-J. Hu, R. Thomale, D. Poilblanc, and F. Becca, ArXiv e-prints (2016), 1601.06018.
- ⁶³ W. Zheng, J.-W. Mei, and Y. Qi, ArXiv e-prints (2015), 1505.05351.
- ⁶⁴ Y.-M. Lu, ArXiv e-prints (2015), 1505.06495.
- ⁶⁵ Y. Zhang, T. Grover, and A. Vishwanath, Phys. Rev. B **84**, 075128 (2011), URL <http://link.aps.org/doi/10.1103/PhysRevB.84.075128>.
- ⁶⁶ Y. Zhang, T. Grover, A. Turner, M. Oshikawa, and A. Vishwanath, Phys. Rev. B **85**, 235151 (2012), URL <http://link.aps.org/doi/10.1103/PhysRevB.85.235151>.
- ⁶⁷ Y. Zhang and A. Vishwanath, Phys. Rev. B **87**, 161113 (2013), URL <http://link.aps.org/doi/10.1103/PhysRevB.87.161113>.
- ⁶⁸ X.-G. Wen, Phys. Rev. B **65**, 165113 (2002), URL <http://link.aps.org/doi/10.1103/PhysRevB.65.165113>.
- ⁶⁹ S. Bieri, C. Lhuillier, and L. Messio, ArXiv e-prints (2015), 1512.00324.
- ⁷⁰ S. Sorella, Phys. Rev. B **71**, 241103 (2005), URL <http://link.aps.org/doi/10.1103/PhysRevB.71.241103>.
- ⁷¹ L. Messio, C. Lhuillier, and G. Misguich, Phys. Rev. B **83**, 184401 (2011), URL <http://link.aps.org/doi/10.1103/PhysRevB.83.184401>.
- ⁷² Q. Niu, D. J. Thouless, and Y.-S. Wu, Phys. Rev. B **31**, 3372 (1985), URL <http://link.aps.org/doi/10.1103/PhysRevB.31.3372>.
- ⁷³ D. N. Sheng, X. Wan, E. H. Rezayi, K. Yang, R. N. Bhatt, and F. D. M. Haldane, Phys. Rev. Lett. **90**, 256802 (2003), URL <http://link.aps.org/doi/10.1103/PhysRevLett.90.256802>.
- ⁷⁴ X. Wan, D. N. Sheng, E. H. Rezayi, K. Yang, R. N. Bhatt, and F. D. M. Haldane, Phys. Rev. B **72**, 075325 (2005), URL <http://link.aps.org/doi/10.1103/PhysRevB.72.075325>.
- ⁷⁵ M. Hafezi, A. S. Srensen, M. D. Lukin, and E. Demler, EPL (Europhysics Letters) **81**, 10005 (2008), URL <http://stacks.iop.org/0295-5075/81/i=1/a=10005>.